Role of Mg^{2+} and Ca^{2+} in DNA Bending: Evidence from an ONIOM-Based QM-MM Study of a DNA Fragment

Neethu Sundaresan,[†] C. K. S. Pillai,[†] and Cherumuttathu H. Suresh*[,‡]

Polymer Chemistry Section of the Chemical Sciences Division and Computational Modeling and Simulation Section, Regional Research Laboratory (CSIR), Trivandrum 695 019, India

Received: March 22, 2006; In Final Form: May 11, 2006

The binding of hydrated Mg^{2+} and Ca^{2+} ions with a DNA fragment containing two phosphate groups, three sugar units, and a G·C base pair is modeled in the anion and dianion states using a three-layer ONIOM approach. A monodentate binding mode was the most stable structure observed for both the ions in the anion model. However, the interactions of Mg^{2+} and Ca^{2+} with the dianion model of the DNA fragment gave rise to a large structural deformation at the base pair region, leading to the formation of "ring" structures. In both anion and dianion models, Mg^{2+}-bound structures were considerably more stable than the corresponding Ca^{2+}-bound structures. This feature and the formation of ring structures in the dianion models strongly supported the higher coordination power of the Mg^{2+} toward DNA systems for its compaction. The charge of the DNA fragment appeared to be crucial in deciding the binding strength as well as the binding mechanism of the metal ions. To the best of our knowledge, this is the first theoretical investigation of the interaction of a comparatively larger DNA model system with the biologically important Mg^{2+} and Ca^{2+} ions.

Introduction

DNA−metal ion interactions play key roles in the control of DNA conformation and its topology.[1−7] These interactions are governed by several parameters such as the nature of the metal, its size, and its charge.[8−12] All these parameters influence the conformation of DNA by direct or indirect interaction through the water molecules with the basic sites of the nucleotides.[13] Although monovalent cations have been found in a few cases to be localized at preferred binding sites of DNA with low occupancies, the stable and specific solvation geometries adopted by divalent cations endow them with the ability to strongly and selectively bind DNA.[14−17] For instance, coordination of phosphate moieties by alkaline-earth cations such as Mg^{2+} and Ca^{2+} is essential in folding and winding of the polynucleic acids as they assume compact arrangements in vivo[18] for catalytic enzymatic reactions involving de-esterification of phosphate esters,[19,20] stabilization of triple and quadruple helices, for the processes involving the transfer of genetic information and the synthesis of oligonucleotides.[21]

Theoretical studies performed by Sponer et al.[22−27] on small model systems such as base pair nucleotides and solvated metal ions and by Petrov and co-workers[28−30] on dimethyl phosphate anion and works by other groups[31−38] have shed new light on binding of metal to nucleic acids. In native DNA, the electronegative oxygen atoms of the phosphate group are usually projected toward the exterior of the double helix and the small models are largely ineffective in replicating such geometrical constraints. Moreover, a model containing dimethyl phosphate anion and a dication gives a net positive charge on the system which is perhaps unrealistic because one would expect either neutralized or excess negative charge on DNA. This has prompted us to investigate the effect of excess electrons on the properties of binding of divalent cations to a DNA fragment where the phosphate groups are projected toward the exterior. Here, we address the computational analysis using a QM-MM approach to understand the relationship between molecular structures and energies of a DNA fragment containing a guanine· cytosine base pair and the connected sugar and phosphate moieties.

SCHEME 1

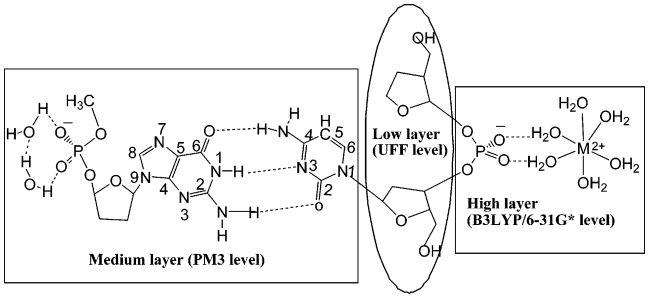

Computational Details and Models

Scheme 1 gives the dianion model of the DNA fragment interacting with the hexahydrated metal dication in the outer sphere binding mode. This model is designated as $(H_2O)_2-^{-}$ PSG−CSP^{-}−M^{2+}, where P, S, G, and C represent the phosphate, sugar, guanine, and cytosine moieties, respectively, and M^{2+} represents a hexahydrated dication. To avoid a bare phosphate group in the system, the water dimer is used as a microsolvation model. We will be utilizing a three-layer ONIOM method, developed by Morokuma and co-workers,[39−41] as the QM-MM technique in studying the interactions of the metal ion with the DNA segment. ONIOM is a general hybrid method which can combine both molecular orbital and molecular mechanics methods, and it is now becoming an effective and

* To whom correspondence should be addressed. Fax: +91-471-2491712. Phone: +91-471-2515264. E-mail: sureshch@gmail.com.
† Polymer Chemistry Section of the Chemical Sciences Division.
‡ Computational Modeling and Simulation Section.

10.1021/jp061774q CCC: $33.50 © 2006 American Chemical Society
Published on Web 06/15/2006

SCHEME 2

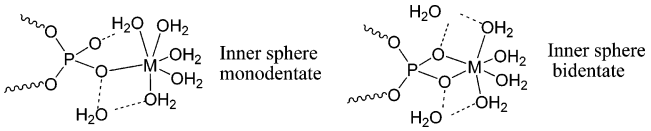

indispensable tool for studying the chemical structure and reactivity of large molecular systems.[42,43]

According to the ONIOM terminology, the $(H_2O)_2-^-PSG-CSP^--M^{2+}$ model is divided into three layers: (i) a high layer, (ii) a medium layer, and (iii) a low layer (illustrated in Scheme 1). The hexahydrated structure of the metal is chosen for the high layer because it is the most commonly observed primary solvation shell of Mg^{2+} and Ca^{2+}. Since DNA phosphate−metal ion interaction is the main focus of this work, the hydrated metal and phosphate anion was treated at the highest level of theory. Therefore, it is expected that for the high layer, the critical parts of the reacting system can be relatively and accurately described using DFT calculation at the B3LYP level[44,45] in conjunction with the standard 6-31G(d) basis set. As the second objective of the work is to study the effect of metal ion−phosphate interaction on the G·C base pair, the G·C base pair, the sugar units, and phosphate group at the guanine end were treated at the medium level (PM3) of theory.[46] The PM3 method is a well-parametrized and widely used semiempirical method for obtaining reliable geometries of organic systems, and therefore, we expect that the structural features obtained with this method will be quite reasonable for the medium layer. In addition, the use of the PM3 method will incorporate some electronic effects into the system, leading to some charge delocalization from the anionic phosphate moieties. The low layer of the system is the MM layer because to model this layer we used the UFF force field.[47] This force field is particularly useful in treating the steric effect imposed by the sugar unit, and by doing so, we can prevent the direct electronic interaction between the QM layer and the medium layer which in turn will help the phosphate moiety to the exterior of the DNA fragment. Therefore, we expect that the three-layer ONIOM method adopted in this work would give reliable results as it provides a compromise between accuracy and applicability to large systems.[48−50]

In addition to the outer sphere binding mode given in Scheme 1, we have also studied the inner sphere mono- and bidentate binding modes (Scheme 2). In these models, one or two water molecules will have to move out from the hexahydration shell (one for monodentate and two for bidentate) to make room for the direct metal−phosphate oxygen bonds. Further, an anion model is also studied to compare the results obtained from the dianion model. In the anion model, the two water molecules in the medium layer are replaced with a proton on the oxygen, and it is labeled as $HPSG-CSP^--M^{2+}$. Anion $HPSG-CSP^-$ and dianion $^-PSG-CSP^-$ structures without the hexahydrated metal ions were also located. All the optimized structures were subjected to full energy calculation at the B3LYP/6-31G* level of theory. The basis set superposition error (BSSE) was incorporated in the interaction energy calculation by using the counterpoise method of Boys and Bernardi.[51] The BSSE-corrected interaction energy is used in comparing the stability of different structures.

Results and Discussion

$HPSG-CSP^--M^{2+}$ Anion Models. The ONIOM level optimization of the anion models gave outer sphere, inner sphere monodentate, and inner sphere bidentate structures for Mg^{2+} and outer sphere and inner sphere monodentate structures for Ca^{2+}. All attempts to find an inner sphere bidentate structure for Ca^{2+} have failed. In both metal ions, the most stable structure was found to be the inner sphere monodentate form, and these are depicted in panels A and B of Figure 1 for Mg^{2+} and Ca^{2+}, respectively. The structures were very similar to each other, and the most significant difference between them was in their average O−H hydrogen bond lengths observed in the hydration region. Compared to a shorter O−H value of 1.788 Å in the Mg^{2+} system, a significantly large O−H value of 1.928 Å is found in the Ca^{2+} system. Similarly, compared to the average Mg−O distance of 2.103 Å, a larger value of 2.419 Å is observed for the average Ca−O distance, which may be attributed to the larger ionic radius of Ca^{2+} as compared to the Mg^{2+} ion. These results indicate a stronger affinity of the hydrated Mg^{2+} versus that of hydrated Ca^{2+} in binding with the phosphate moiety of the DNA fragment.

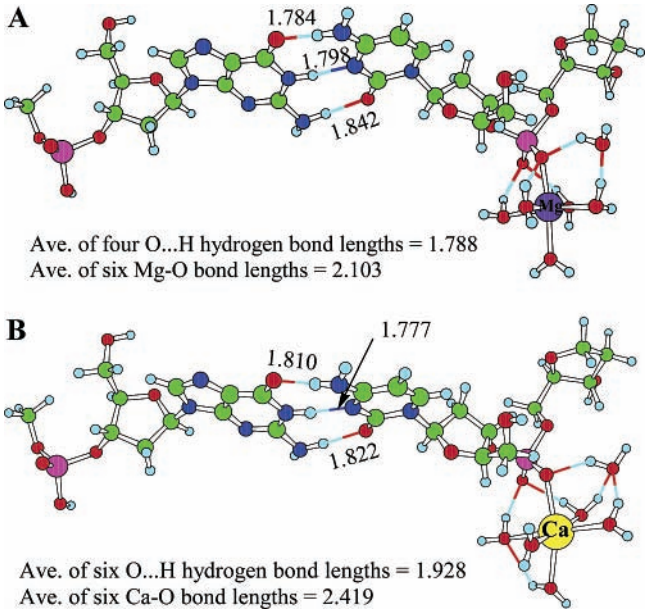

Figure 1. Inner sphere monodentate anion models of (A) Mg^{2+} and (B) Ca^{2+} binding. All bond lengths are in angstroms.

Although our main focus of the study is the DNA phosphate−metal ion interaction, the ONIOM models used in this work can also shed light on the stability of the G·C base pair in the anion, dianion, and their metal-containing systems. For example, the distances observed for the ordered triplet [$O6_{(G)}-N4_{(C)}$, $N1_{(G)}-N3_{(C)}$, and $N2_{(G)}-O2_{(C)}$] in the G·C base pair for free anion and dianion models are 2.820, 2.804, and 2.828 Å and 2.810, 2.816, and 2.850 Å, respectively, suggesting that the $N1_{(G)}-N3_{(C)}$ and $N2_{(G)}-O2_{(C)}$ interactions in the dianion model are weaker than that found in the anion model (for more structural features, see the Supporting Information). Therefore, a slight weakening of the G·C base pair interaction was expected in the dianion system, and this can be attributed to the enhanced electrostatic repulsive interaction arising from anionic guanine and cytosine ends. The $O6_{(G)}-N4_{(C)}$, $N1_{(G)}-N3_{(C)}$, and $N2_{(G)}-O2_{(C)}$ distances in the anion and dianion models can also be compared with corresponding values in the free G·C base pair. For instance, for the free G·C base pair optimized at the PM3 level, $O6_{(G)}-N4_{(C)}$, $N1_{(G)}-N3_{(C)}$, and $N2_{(G)}-O2_{(C)}$ distances of 2.813, 2.800, and 2.850 Å, respectively, were obtained and were very close to the corresponding values obtained for the anion and dianion models. In the anion and dianion models, and also in the free G·C base pair optimized at the PM3 level, the aromatic rings of the guanine and cytosine moieties were located

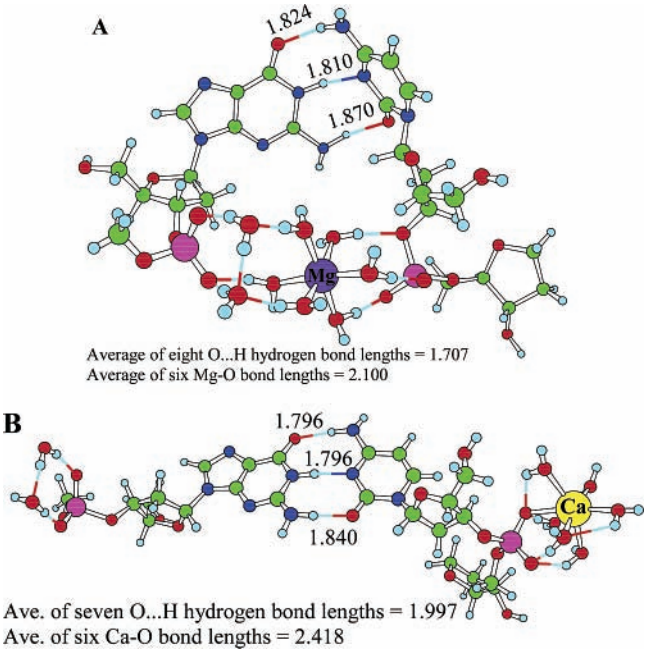

Figure 2. Dianion models. (A) Outer sphere binding of Mg^{2+} and (B) inner sphere monodentate binding of Ca^{2+}. All bond lengths in angstroms.

nearly in the same plane. In fact, the structural features of the G·C base pair obtained at the PM3 level were in good agreement with those of the G·C base pair structure obtained by Sponer et al. at the RI-MP2/TZVPP level [a planar structure with an $O6_{(G)}-N4_{(C)}$ distance of 2.750 Å, an $N1_{(G)}-N3_{(C)}$ distance of 2.900 Å, and an $N2_{(G)}-O2_{(C)}$ distance of 2.891 Å].[52] Therefore, we felt that the three-layer ONIOM method used in this work is adequate for the model studies on the DNA fragment systems.

$(H_2O)_2-^{-}PSG-CSP^{-}-M^{2+}$ Dianion Models. For the dianion models, outer sphere and inner sphere monodentate structures were identified as the most stable binding modes of Mg^{2+} and Ca^{2+}, respectively (Figure 2A,B). The inner sphere monodentate and inner sphere bidentate structures were also identified for Mg^{2+}. A structure search for the outer sphere and the inner sphere bidentate binding modes of Ca^{2+} always gave the inner sphere monodentate structure. The most interesting phenomenon occurred in the case of Mg^{2+}, where the otherwise linear fragment became bent into ringlike structures in all three binding modes that were studied. Here, the Mg^{2+} binds to the cytosine end phosphate group in an outer sphere manner and to the guanine end phosphate group via water-mediated hydrogen bonds.

It may be noted that in optimizing these "ring" structures, we always started with a structure in which both phosphate moieties were far apart, and these initial geometries were structurally very similar to the structures in Figures 1A,B and 2B. The structures in Figures 1A,B and 2B can be called "linear" structures on the basis of the linear arrangement of hydrogen-bonded atoms in their G·C base pair. In the case of Mg^{2+} dianion models, the optimization starting from a linear structure never converged back to such a structure, and it went all the way to the ring structure. However, in the case of Ca^{2+}, starting from a linear structure, we found the optimization always gave the linear structure.

In contrast to the linear monodentate binding mode of Mg^{2+} in the anion model, the ring structures of its dianion models preferred an outer sphere binding. On the other hand, Ca^{2+} ion preferred the inner sphere monodentate binding mode in both

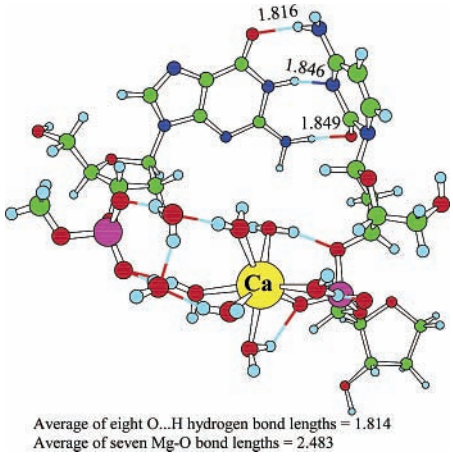

Figure 3. Dianion model showing the inner monodentate binding of Ca^{2+} in the ring structure. All bond lengths are in angstroms.

the anion and dianion linear models. The absence of linear structures and the identification of ring structures in all the dianion models of Mg^{2+} (outer, inner monodentate, and inner bidentate) point toward its higher coordinating power and, hence, DNA bending ability compared to those of Ca^{2+}. The drastic structural change of the DNA fragment observed after the interaction of Mg^{2+} with the dianion model further suggests that the mode of binding of the metal ion to DNA largely depends on the charge of the DNA fragment. These results also suggest that the typically used model of anion−dication combination giving a net positive charge is inadequate for understanding the proper binding behavior of the metal ion with DNA systems.

Since the automatic generation of ring structures from linear starting structures did not succeed in the optimization of dianion models with Ca^{2+} ion, we also attempted the geometry optimization by first constructing a ring structure as the initial guess geometry for the outer, inner monodentate, and inner bidentate coordination mode of hydrated Ca^{2+}. However, this procedure gave only an inner sphere monodentate structure for it. The optimization for the outer sphere converged to the inner sphere monodentate form, and for the bidentate structure, the optimization did not give a meaningful structure. The optimized inner sphere monodentate ring structure is presented in Figure 3.

It should be noted that in the cell nucleus, the double-helical DNA molecule which is quite long (up to several meters in some organisms) is compactly arranged in the very small confined region (which is far smaller than the length of the DNA molecule) of the cell nucleus, which is possible only through bending and winding of long DNA molecules. DNA bending is believed to occur by its intrastrand or interstrand interaction of the phosphate and/or base (water-mediated or non-water-mediated) with cationic species, including metal ions present in the cell. Since the present models do not have two phosphate groups on the same strand of DNA, Mg^{2+} and Ca^{2+} could not interact with the phosphate group in an intrastrand manner but could establish interstrand phosphate bridging which eventually led to the formation of ring structure. The important point is that, even at this extreme conformation, the G·C base pair region exhibited a substantial amount of stabilizing hydrogen bond interaction.

Compared to the average O−H hydrogen bond length of 1.788 Å observed in the metal ion hydration region in the anion model of Mg^{2+}, the corresponding value in the dianion model (ring structure) is significantly shorter (1.707 Å). This suggests

a stronger metal−phosphate interaction in the dianion model than in the anion model, and this may be attributed to simultaneous interaction of the hydrated metal ion with the two phosphate groups, leading to a well-balanced charge neutralization in the system. On the other hand, the charge is well-separated in the linear Ca^{2+} dianion structure (negative charge at the guanine end and net positive charge at the cytosine end), which in turn exhibited longer O−H hydrogen bond lengths (1.997 Å) than the anion model (1.928 Å). Like the dianion model of Mg^{2+} ring structures, the Ca^{2+} ring structures also exhibited a significantly shorter average O−H hydrogen bond length (1.814 Å) compared to that in the anion systems, which again points toward the importance of the simultaneous interaction of two phosphate groups to a dication (for other structures and bond length information, see the Supporting Information).

Another observation is that the anion and dianion models showed nearly the same average metal−oxygen distance for Mg^{2+} as well as linear structures of Ca^{2+} ions. However, in the case of the ring structure of Ca^{2+}-induced dianion systems, the average Ca−O distance of 2.483 Å is 0.064 Å larger than that found in the anion system. This difference may be attributed to the seven Ca−O bonds found in the ring structure (Figure 2) compared to six metal−O distances in all other systems. Ca^{2+} has a larger coordination sphere than Mg^{2+}, and therefore in the monodentate dianion coordination, it was able to retain the bonding interaction with all six water molecules as well as the metal−phosphate oxygen bond. This may be the reason for the absence of an outer sphere structure for the Ca^{2+}-induced dianion systems.

The marked differences in the Mg^{2+} and Ca^{2+} binding modes have been reported in the experimental work of Tajmir-Riahi[53] where he noticed direct binding of Ca^{2+} and indirect binding of Mg^{2+} to phosphates. Further support for the results presented here can be found in another study, where it was proven that Mg^{2+} binds to DNA in an outer sphere (water-mediated) manner, while larger cations, Ca^{2+}, Sr^{2+}, and Ba^{2+}, bind to DNA in an inner sphere (direct contact) manner, which can be correlated with the hydration energies of the cations. Outer sphere complexes for Mg^{2+}−DNA were also suggested from ^{31}P NMR and crystallographic studies.[54] One should also point out the recent study on CGCGAATTCGCG, GGCGAATTCGCG, and GCGAATTCGCG crystals in the presence of Mg^{2+} and Ca^{2+} ions.[55] This work revealed that Mg^{2+} binds to the oligonucleotides in an outer sphere manner while Ca^{2+} is engaged in more inner sphere complexes.

It has been seen that an anion−dication model of Mg^{2+} preferred the inner sphere monodentate binding mode while its dianion−dication model preferred the outer sphere coordination. The latter case is more realistic due to the net charge of zero on the system and also is in agreement with the experimental findings. For inner sphere coordinations of Mg^{2+}, removal of water molecules from the primary solvation shell is necessary, and this in turn decreases the binding energy, which may be attributed to the small size of the cation. In all the models used for Ca^{2+}, the inner sphere monodentate structure is the most stable, and this result also supported the experimental findings. The seven Ca−O bonds found in the more realistic dianion−dication ring structure model of Ca^{2+} suggest that the cation size is an important factor in deciding the binding mechanism.

Interaction Energies. Other than the structural features, the models used in this study can also give us valuable information about the G·C base pair and metal ion−phosphate interaction energies. Equations 1−6 have been constructed for various interaction energies.

For G·C base pair interaction energy in the free anion

$$E_1 = E(HPSG) + E(CSP^-) - E(\mathrm{HPSG{-}CSP^-}) + E_{1\mathrm{BSSE}} \quad (1)$$

For G·C base pair interaction energy in the free dianion

$$E_2 = E((H_2O)_2{-}{}^-PSG) + E(CSP^-) - E((\mathrm{H_2O})_2{-}{}^-\mathrm{PSG{-}CSP^-}) + E_{2\mathrm{BSSE}} \quad (2)$$

For G·C base pair interaction energy in the metal-bound anion systems

$$E_3 = E(HPSG) + E(CSP^-{-}M^{2+}) - E(\mathrm{HPSG{-}CSP^-{-}M^{2+}}) + E_{3\mathrm{BSSE}} \quad (3)$$

For G·C base pair interaction energy in the metal-bound dianion linear systems

$$E_4 = E((H_2O)_2{-}{}^-PSG) + E(CSP^-{-}M^{2+}) - E((\mathrm{H_2O})_2{-}{}^-\mathrm{PSG{-}CSP^-{-}M^{2+}}) + E_{4\mathrm{BSSE}} \quad (4)$$

For metal ion−phosphate interaction energy in the anion systems

$$E_5 = E(\mathrm{HPSG{-}CSP^-}) + E(\mathrm{M^{2+}}) - E(\mathrm{HPSG{-}CSP^-{-}M^{2+}}) + E_{5\mathrm{BSSE}} \quad (5)$$

For hydrated metal ion−phosphate interaction energy in the dianion systems

$$E_6 = E((\mathrm{H_2O})_2{-}{}^-\mathrm{PSG{-}CSP^-}) + E(\mathrm{M^{2+}}) - E((\mathrm{H_2O})_2{-}{}^-\mathrm{PSG{-}CSP^-{-}M^{2+}}) + E_{6\mathrm{BSSE}} \quad (6)$$

The E values on the right-hand side of the equations are the total energy calculated at the B3LYP/6-31G* level for the systems given in parentheses. Names in regular font are of fully optimized ONIOM level structures, and those in italics are of the fragment structures taken from the fully optimized systems. $E_{1\mathrm{BSSE}}$−$E_{6\mathrm{BSSE}}$ are the BSSE corrections obtained by employing the counterpoise correction method of Boys and Bernardi.[51] In the dianion ring structures, because the metal ion is interacting simultaneously with both phosphate anion moieties, a reasonable estimate of the G·C base pair interaction is not possible, and therefore, it will not be discussed. $E(\mathrm{M^{2+}})$ in eqs 5 and 6 is the energy value of the optimized octahedral structure of the hexahydrated metal ion at the B3LYP/6-31G* level (see the Supporting Information for their geometries).

The BSSE-corrected G·C base pair interaction energy is found to be 29.6 (E_1) and 7.3 kcal/mol (E_2) for the metal free anion and dianion models, respectively. According to the calculations of Sponer et al.,[52] the interaction energy (E_{int}) for a neutral G·C base pair obtained with RI-MP2/aug-cc-pVTZ level calculations was 27.0 kcal/mol. Thus, the value obtained for the bare anion model was 2.6 kcal/mol higher and for the dianion model 19.7 kcal/mol lower. This result is not surprising because the anion model can be visualized as the interaction between the neutral guanine fragment and the anionic cytosine fragment, and the energy of this type of a neutral−charged interaction is expected be higher than that of the neutral−neutral interaction found in a free G·C base pair. On the other hand, the electrostatic repulsion between the negatively charged guanine [$(H_2O)_2{-}{}^-$PSG] and the negatively charged cytosine (CSP^-) fragments in

TABLE 1: G·C Base Pair Interaction Energy in Anion (E_3) and Dianion (E_4) Models[a]

	outer sphere		inner sphere monodentate		inner sphere bidentate	
	E_3 (anion)	E_4 (dianion)	E_3 (anion)	E_4 (dianion)	E_3 (anion)	E_4 (dianion)
Mg^{2+}	22.9 (4.4)	ring structure	22.6 (4.4)	ring structure	22.3 (4.5)	ring structure
Ca^{2+}	21.7 (4.4)	not found	22.0 (4.4)	34.1 (4.6)	not found	not found

[a] Values in parentheses are the BSSE corrections. All values are in kilocalories per mole.

TABLE 2: Phosphate-Hydrated Metal Ion Interaction Energies in Anion (E_5) and Dianion (E_6) Models[a]

	outer sphere		inner sphere monodentate		inner sphere bidentate	
	E_5 (anion)	E_6 (dianion)	E_5 (anion)	E_6 (dianion)	E_5 (anion)	E_6 (dianion)
Mg^{2+}	175.2 (8.7)	315.7 (14.5)	185.4 (11.3)	304.2 (16.9)	180.8 (15.2)	295.8 (15.2)
Ca^{2+}	166.2 (10.2)	not found	178.5 (12.3)	216.3 (14.6),[b] 286.1 (17.4)[c]	not found	not found

[a] Values in parentheses are the BSSE corrections. All values are in kilocalories per mole. [b] Linear structure. [c] Ring structure.

the dianion model will induce repulsive electrostatic interaction, and therefore, a significant reduction in the E_{int} value is observed in its G·C base pair interaction.

As we can see from the E_3 values given in Table 1, in the case of an anion model containing a metal ion (HPSG−CSP$^-$−M^{2+}), both metal ions exhibit nearly the same G·C base pair interaction energy which is in the range of 21.7−22.9 kcal/mol. This suggests that the interaction of the hydrated metal with the phosphate anion reduces the hydrogen bond strength in the G·C region by ∼7.2 kcal/mol. This reduction is quite significant because this value is approximately 26% of the G·C base pair interaction energy in the free anion system. On the other hand, in the case of the linear dianion model of Ca^{2+} (inner sphere monodentate), the G·C base pair interaction energy of 34.1 kcal/mol was quite high when compared to the corresponding value found in the metal free dianion system. This result is not surprising because in the linear dianion system, strong electrostatic interaction in the G·C region is expected because the dianion system can be considered as the interaction between the negatively charged $(H_2O)_2$−$^-$PSG form and the positively charged CSP$^-$−Ca^{2+} form which in a sense is an anion−cation interaction. It is expected that even in the dianion ring structures of Mg^{2+} and Ca^{2+}, a substantial amount of G·C base pair interaction energy is expected because in all these systems, the $O6_{(G)}$−$N4_{(C)}$, $N1_{(G)}$−$N3_{(C)}$, and $N2_{(G)}$−$O2_{(C)}$ hydrogen bond lengths were all well within the bonding region. For all the E_1−E_4 energy calculations, the BSSE correction is found to be nearly constant (4.4−4.6 kcal/mol).

Interaction energies E_5 and E_6 reported in Table 2 can be considered as a good measure of how strongly the hydrated metal ion binds with the phosphate groups. In both anion and dianion models, the binding of Mg^{2+} to the phosphate groups is stronger than the binding of Ca^{2+}. The binding energies of 185.7 and 178.5 kcal/mol are observed for the most stable inner sphere monodentate anion models of both Mg^{2+} and Ca^{2+}, respectively. Very recently, Petrov and co-workers[28] studied the dimethyl phosphate anion systems with Mg^{2+} and Ca^{2+} and obtained values of 204.3 and 198.3 kcal/mol, respectively, for the monodentate structures. Although the model presented here and the Petrov model are markedly different, the smaller value obtained in our case can be attributed mainly to the weakening of the G·C base pair interaction. The drastic structural change observed in the dianion models of Mg^{2+} is also reflected in their interaction energies. All three bent structures of Mg^{2+} exhibited a substantial increase in their interaction energy as compared to the anion systems, and a maximum increase of 80.3% is observed in the most stable outer sphere dianion structure. On the other hand, the linear monodentate Ca^{2+} dianion structure exhibited an increase of 21.2% in the interaction energy compared to that of the anion structure. The high interaction energy of 315.7 kcal/mol observed for the Mg^{2+} outer sphere structure is attributed to the simultaneous interaction of the ion with both phosphate groups. Further, this stabilization energy was 29.6 kcal/mol higher than that of the dianion ring structure of Ca^{2+}. In the ring structures, the interaction of the metal with phosphate groups is so dominant that the structural deformation leading to the weakening of the G·C base pair interaction is well-compensated. In the calculation of E_5 and E_6, the BSSE correction was found to be in the range of 8.7−17.4 kcal/mol.

Conclusions

The interactions of hydrated Mg^{2+} and Ca^{2+} ions with the phosphate group of a DNA are studied by modeling a DNA fragment in an anion (one negative charge) and dianion (two negative charges) state with the phosphate geometry maintained as in native DNA (projected toward the exterior) using a three-layer ONIOM-based QM-MM method. Three combinations of metal ion−DNA binding were studied: the outer sphere, inner sphere monodentate, and inner sphere bidentate patterns. In the anion model, both ions preferred the inner sphere monodentate binding mechanism. However, in the case of the dianion model, the metal ions induced major structural changes in the system, by bending the linear DNA fragment into stable ringlike structures. Mg^{2+}-bound ring structures were more stable than those with Ca^{2+} ion by 29.6 kcal/mol; on the other hand, Mg^{2+} preferred outer sphere and Ca^{2+} preferred the inner sphere monodentate binding pattern. Our results indicate that unlike that of the Ca^{2+} ion, the pattern of binding of Mg^{2+} to DNA largely depends on the charge of the DNA fragment and also gives a clue about the biological roles of these metal ions in DNA bending. The binding of hydrated Mg^{2+} and Ca^{2+} ions to the dianion model of DNA revealed a more realistic picture of DNA−alkaline-earth metal interactions in the cell compared to the anion model which is in good agreement with the previous experimental reports.

Acknowledgment. Financial support of CSIR to N.S. is gratefully acknowledged.

Supporting Information Available: Three-dimensional structure and Cartesian coordinates for the ONIOM level optimized geometries of all the molecules. This material is available free of charge via the Internet at http://pubs.acs.org.

References and Notes

(1) Rouzina, I.; Bloomfield, V. A. *Biophys. J.* **1998**, *74*, 3152.
(2) Egli, M. *Curr. Opin. Chem. Biol.* **2004**, *8*, 580.

(3) Egli, M. *Chem. Biol.* **2002**, *9*, 277.
(4) Subirana, J. A.; Soler-Lopez, M. *Annu. Rev. Biophys. Biomol. Struct.* **2003**, *32*, 27.
(5) Stellwagen, N. C.; Mohanty, U. Curvature and deformation of nucleic acids: Overview. In *Nucleic Acids: Curvature and Deformation*; American Chemical Society: Washington, DC, 2004; Vol. 884, p 1.
(6) Maher, L. J. *Curr. Opin. Chem. Biol.* **1998**, *2*, 688.
(7) Hardwidge, P. R.; Pang, Y. P.; Zimmerman, J. M.; Vaghefi, M.; Hogrefe, R.; Maher, L. J. Phosphate crowding and DNA bending. In *Nucleic Acids: Curvature and Deformation*; American Chemical Society: Washington, DC, 2004; Vol. 884, p 111.
(8) Rueda, M.; Cubero, E.; Laughton, C. A.; Orozco, M. *Biophys. J.* **2004**, *87*, 800.
(9) Anastassopoulou, J. *J. Mol. Struct.* **2003**, *651*, 19.
(10) Sletten, E.; Froystein, N. A. MMR studies of oligonucleotide-metal ion interactions. In *Metal Ions in Biological Systems*; Marcel Dekker: New York, 1996; Vol. 32, p 397.
(11) McFail-Isom, L.; Sines, C. C.; Williams, L. D. *Curr. Opin. Struct. Biol.* **1999**, *9*, 298.
(12) McConnell, K. J.; Beveridge, D. L. *J. Mol. Biol.* **2000**, *304*, 803.
(13) Missailides, S.; Anastassopoulou, J.; Fotopoulos, N.; Theophanides, T. *Asian J. Phys.* **1997**, *6*, 481.
(14) Duguid, J. G.; Bloomfield, V. A.; Benevides, J. M.; Thomas, G. J. *Biophys. J.* **1995**, *69*, 2623.
(15) Christianson, D. W. *Prog. Biophys. Mol. Biol.* **1997**, *67*, 217.
(16) Glusker, J. P. *Adv. Protein Chem.* **1991**, *42*, 1.
(17) Holm, R. H.; Kennepohl, P.; Solomon, E. I. *Chem. Rev.* **1996**, *96*, 2239.
(18) Widom, J. *Annu. Rev. Biophys. Biomol. Struct.* **1998**, *27*, 285.
(19) Knowles, J. R. *Annu. Rev. Biochem.* **1980**, *49*, 877.
(20) Bamann, E.; Trapmann, H.; Fischler, F. *Biochem. Z.* **1954**, *328*, 89.
(21) Marzilli, L. G. K. T. J.; Eichhorn, G. L. In *Nucleic Acid-Metal Ion Interactions*; John Wiley and Sons: New York, 1980; Vol. 1.
(22) Sponer, J.; Burda, J. V.; Leszczynski, J.; Hobza, P. *J. Biomol. Struct. Dyn.* **1999**, *17*, 61.
(23) Sponer, J.; Hobza, P. *Collect. Czech. Chem. Commun.* **2003**, *68*, 2231.
(24) Sponer, J.; Leszczynski, J.; Hobza, P. *THEOCHEM* **2001**, *573*, 43.
(25) Sponer, J.; Sabat, M.; Burda, J. V.; Leszczynski, J.; Hobza, P.; Lippert, B. *J. Biol. Inorg. Chem.* **1999**, *4*, 537.
(26) Sponer, J. E.; Sychrovsky, V.; Hobza, P.; Sponer, J. *Phys. Chem. Chem. Phys.* **2004**, *6*, 2772.
(27) Munoz, J.; Sponer, J.; Hobza, P.; Orozco, M.; Luque, F. J. *J. Phys. Chem. B* **2001**, *105*, 6051.
(28) Petrov, A. S.; Funseth-Smotzer, J.; Pack, G. R. *Int. J. Quantum Chem.* **2005**, *102*, 645.
(29) Petrov, A. S.; Lamm, G.; Pack, G. R. *J. Phys. Chem. B* **2002**, *106*, 3294.
(30) Petrov, A. S.; Lamm, G.; Pack, G. R. *J. Phys. Chem. B* **2004**, *108*, 6072.
(31) Bandyopadhyay, D.; Bhattacharyya, D. *J. Biomol. Struct. Dyn.* **2003**, *21*, 447.
(32) Bertran, J.; Rodriguez-Santiago, L.; Sodupe, M. *J. Phys. Chem. B* **1999**, *103*, 2310.
(33) Zeizinger, N.; Burda, J. V.; Sponer, J.; Kapsa, V.; Leszczynski, J. *J. Phys. Chem. A* **2001**, *105*, 8086.
(34) Murashov, V. V.; Leszczynski, J. *J. Phys. Chem. B* **1999**, *103*, 8391.
(35) Rodger, A.; Sanders, K. J.; Hannon, M. J.; Meistermann, I.; Parkinson, A.; Vidler, D. S.; Haworth, I. S. *Chirality* **2000**, *12*, 221.
(36) Marincola, F. C.; Denisov, V. P.; Halle, B. *J. Am. Chem. Soc.* **2004**, *126*, 6739.
(37) Kankia, B. I. *Biopolymers* **2004**, *74*, 232.
(38) Jerkovic, B.; Bolton, P. H. *Biochemistry* **2001**, *40*, 9406.
(39) Svensson, M.; Humbel, S.; Froese, R. D. J.; Matsubara, T.; Sieber, S.; Morokuma, K. *J. Phys. Chem.* **1996**, *100*, 19357.
(40) Humbel, S.; Sieber, S.; Morokuma, K. *J. Chem. Phys.* **1996**, *105*, 1959.
(41) Dapprich, S.; Komaromi, I.; Byun, K. S.; Morokuma, K.; Frisch, M. J. *THEOCHEM* **1999**, *461*−*462*, 1.
(42) Tschumper, G. S.; Morokuma, K. *THEOCHEM* **2002**, *592*, 137.
(43) Re, S.; Morokuma, K. *J. Phys. Chem. A* **2001**, *105*, 7185.
(44) Becke, A. D. *J. Chem. Phys.* **1993**, *98*, 5648.
(45) Becke, A. D. *Phys. Rev. A* **1988**, *38*, 3098.
(46) Stewart, J. J. P. *J. Comput. Chem.* **1989**, *10*, 209.
(47) Rappé, A. K.; Casewit, C. J.; Colwell, K. S.; Goddard, W. A., III; Skiff, W. M. *J. Am. Chem. Soc.* **1992**, *114*, 10024.
(48) Morokuma, K. *Bull. Korean Chem. Soc.* **2003**, *24*, 797.
(49) Roggero, I.; Civalleri, B.; Ugliengo, P. *Chem. Phys. Lett.* **2001**, *341*, 625.
(50) Rungsirisakun, R.; Jansang, B.; Pantu, P.; Limtrakul, J. *J. Mol. Struct.* **2005**, *733*, 239.
(51) Boys, S. F.; Bernardi, F. *Mol. Phys.* **1970**, *19*, 553.
(52) Sponer, J.; Jurecka, P.; Hobza, P. *J. Am. Chem. Soc.* **2004**, *126*, 10142.
(53) Tajmir-Riahi, H. A. *Biopolymers* **1991**, *31*, 101.
(54) McFail-Isom, L.; Shui, X.; Williams, L. D. *Biochemistry* **1998**, *37*, 17105.
(55) Minasov, G.; Tereshko, V.; Egli, M. *J. Mol. Biol.* **1999**, *291*, 83.